Source characterization from ambient measurements of aerosol optical properties

Christopher D. Cappa,[1] Timothy S. Bates,[2] Patricia K. Quinn,[2] and Daniel A. Lack[3,4]

Received 4 May 2009; revised 8 June 2009; accepted 17 June 2009; published 23 July 2009.

[1] A general method to identify air masses impacted by distinct primary aerosol sources from in situ observations of optical properties of atmospheric aerosols is developed theoretically and tested against measurements made during the second New England Air Quality Study (NEAQS 2004) on board the NOAA *R/V Ronald H. Brown*. Distinct events are identified based on the observation of a temporal coherence in the relationship between a measured intensive optical property (i.e., single scatter albedo) and the extensive property of total light absorption of the sub-micron aerosol. We show that this relationship can be used to differentiate between and quantitatively determine properties of the background aerosol and recent inputs of primary aerosol. Additionally, we show that the fraction of aerosol extinction (or aerosol mass) from primary emissions can be estimated from the albedo-absorption relationship. During the NEAQS 2004 study, the primary aerosol was usually found to be highly absorbing, and thus likely to be derived from anthropogenic combustion sources. Overall primary aerosol contributed a relatively small amount (ca. 11%) to the total sub-micron aerosol burden sampled onboard *R/V Ron Brown*. **Citation:** Cappa, C. D., T. S. Bates, P. K. Quinn, and D. A. Lack (2009), Source characterization from ambient measurements of aerosol optical properties, *Geophys. Res. Lett.*, *36*, L14813, doi:10.1029/2009GL038979.

1. Introduction

[2] The direct radiative effect of atmospheric aerosols on climate results from their ability to absorb and scatter light [*Intergovernmental Panel on Climate Change*, 2007]. The primary control on whether aerosols have a net warming or cooling influence is the particle single scatter albedo (ω) relative to the albedo of the underlying surface, where ω is defined as the fraction of total light extinction ($\sigma_{ext} = \sigma_{sca} + \sigma_{abs}$) due to scattering ($\omega = \sigma_{sca}/\sigma_{ext}$), [*Hansen et al.*, 1997]. The extent to which a given particle absorbs or scatters light depends explicitly on the particle composition and mixing state. Light absorbing material at mid-visible wavelengths is derived predominately from primary combustion emissions, while light scattering aerosols are produced from both primary and secondary (gas-to-particle conversion of natural and anthropogenic gaseous precursors) sources [*Ghan and Schwartz*, 2007]. The chemical composition of aerosols is complex and observations effectively integrate over the entire history of a given air mass. This has made it difficult to determine the identity and properties of primary aerosol sources explicitly from *in situ* measurements except in very well defined environments. However, it is differences in the sources and sinks of aerosols which determine the overall particle characteristics and radiative impacts. Thus, to improve predictions of future climate change for different assumed emissions scenarios it is important to have a sound understanding of the contributions of different sources to observed aerosol abundances.

[3] To facilitate interpretation of *in situ* measurements, it is also necessary to identify and differentiate between air masses that are distinct with respect to recent source contributions and mixing with background air, where here background refers to the appropriate regional average. Back trajectory or particle dispersion models are often used to determine the transport history of an air mass [*Draxler and Rolph*, 2003; *Stohl et al.*, 2005]. Here, we develop a tool which allows for the identification of distinct air masses based solely on observations of aerosol optical properties. Furthermore, we assess the potential for this method to extract information about the nature of primary aerosol emissions sources.

2. Observations and Methods

[4] Sub-micron aerosol absorption and scattering were made onboard the NOAA *R/V Ronald H. Brown* at 1-minute resolution in the marine boundary layer during NEAQS 2004 in July and August 2004 off the northeast coast of the United States [*Quinn et al.*, 2006; *Sierau et al.*, 2006]. Both freshly polluted air masses and somewhat aged air masses were observed during the campaign. Scattering was measured at 450, 550 and 700 nm using a nephelometer (TSI, model 3563) and absorption at 467, 530 and 660 nm using a particle soot absorption photometer (Radiance Research); only the measurements at 530 nm are considered here, where the scattering measurements have been wavelength-adjusted as described by *Sierau et al.* [2006].

[5] Comparison of ω_{obs} and σ_{abs}^{obs} indicates that a clear relationship exists between these intensive and extensive observables for numerous time periods (referred to here as "events"). More than 50 events were identified and analyzed (corresponding to 33% of the observations with an average duration of 2.5 hours, see Figure S2), a sampling of which are shown in Figure 1.[1] Individual event relationships

[1]Department of Civil and Environmental Engineering, University of California, Davis, California, USA.
[2]Pacific Marine Environmental Laboratory, NOAA, Seattle, Washington, USA.
[3]Cooperative Institute for Research in Environmental Sciences, University of Colorado, Boulder, Colorado, USA.
[4]Chemical Sciences Division, Earth Systems Research Laboratory, NOAA, Boulder, Colorado, USA.

0094-8276/09/2009GL038979

[1]Auxiliary materials are available in the HTML. doi:10.1029/2009GL038979.

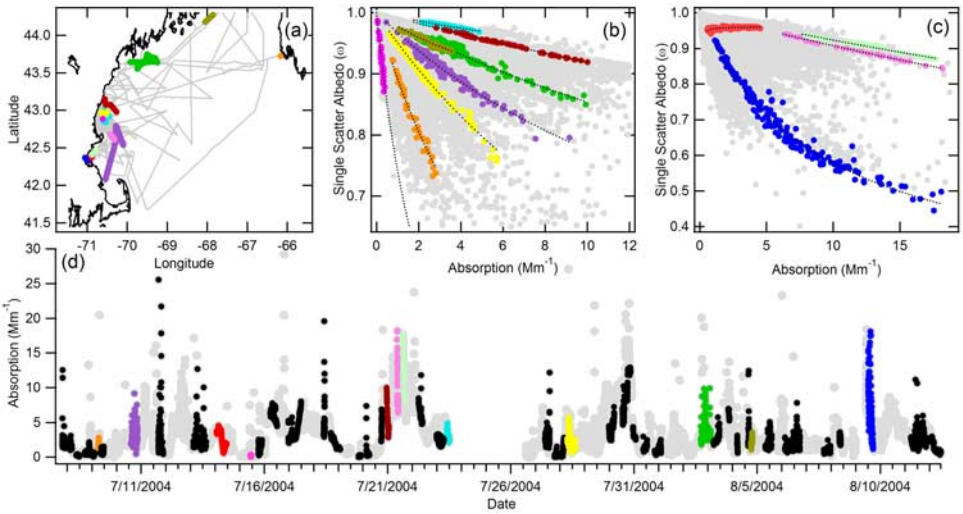

Figure 1. (a) Cruise tracks of the NOAA R/V *Ronald H. Brown* during NEAQS 2004 with individual events highlighted. (b) Variation in the sub-micron ω_{obs} as a function of σ_{abs}^{obs} for a subset of the 50+ identified events. Data for the entire cruise are shown as gray points. Individual events are shown as colored points. (c) Same as Figure 1b but for events specifically identified as having a biomass burning component (red, pink or green) or where ship emissions from Boston Harbor were a significant source of aerosol (blue). Note the different axes in Figures 1b and 1c. (d) The time-series of aerosol light absorption. Data from the entire cruise are shown in gray and identified events in black or color. The colors in the time-series correspond to Figures 1a–1c.

are likely linked to specific aerosol source mixing scenarios which have clearly definable inputs of primary aerosol, while event timescale is determined by a combination of atmospheric dynamics and movement of the ship.

[6] Initial understanding of these relationships comes from simulations using the Lagrangian particle dispersion model FLEXPART [*Stohl et al.*, 2005]. FLEXPART has been previously used to identify NEAQS 2004 aerosol source regions using so-called footprint-layer (150 m) potential emissions sensitivities (PES) [*Quinn et al.*, 2006]. The footprint PES can be used to evaluate whether temporally contiguous events show strong shifts in the air mass history or whether their identification derives from more subtle changes in the source or background air. Examination of the footprint PES' qualitatively indicate that adjacent events tend to either show small, but noticeable, differences in the level of interaction with a source (i.e., Boston) or clear shifts in the background location.

[7] The relationship between ω_{obs} and σ_{abs}^{obs} can be understood quantitatively by considering, for example, the theoretical case where an aged regional background air mass moves over a pollution source shortly before arriving at a receptor site. In this case, the observed aerosol optical properties can be described as having contributions from the regional background aerosol, primary aerosol from the recent pollution source and *in situ* formation of secondary aerosol. Note that secondary aerosol formed from gas-phase precursors co-emitted from the pollution source and those already in the air mass are not distinguished. Similarly, we could consider the mixing of two air masses with distinct aerosol properties. In either case, the observed single scatter albedo at the receptor site is:

$$\omega_{obs} = \frac{\sigma_{sca}}{\sigma_{sca} + \sigma_{abs}} = \frac{\sigma_{sca}^{B} + \sigma_{sca}^{P} + \sigma_{sca}^{S}}{\sigma_{sca}^{B} + \sigma_{sca}^{P} + \sigma_{sca}^{S} + \sigma_{abs}^{B} + \sigma_{abs}^{P}}, \quad (1)$$

where the superscript B, P and S represent the regional background, primary and secondary contributions, and we have assumed that secondary aerosol is non-absorbing (at mid-visible wavelengths). Alternatively, equation (1) can be expressed as:

$$\omega_{obs} = \frac{\sigma_{sca}^{B}\left(\frac{\omega_B - \omega_P}{(1-\omega_P)\omega_B}\right) + \sigma_{sca}^{S} + \left(\frac{\omega_P}{1-\omega_P}\right)\sigma_{abs}^{obs}}{\sigma_{sca}^{B}\left(\frac{\omega_B - \omega_P}{(1-\omega_P)\omega_B}\right) + \sigma_{sca}^{S} + \left(\frac{1}{1-\omega_P}\right)\sigma_{abs}^{obs}} \quad (2)$$

where $\sigma_{abs}^{obs} = \sigma_{abs}^{P} + \sigma_{abs}^{B}$ (see auxiliary material for a derivation of equation (2)). The relationship between ω_{obs} and σ_{abs}^{obs} is non-linear and depends on four fit parameters; ω_B, ω_P, σ_{sca}^{B} and σ_{sca}^{S}. Within this framework, a strong correlation between ω_{obs} and σ_{abs}^{obs} indicates periods with distinct primary source or regional background air contributions and provides direct information on the aerosol properties, in particular of their single scatter albedo. Here, this relationship is briefly explored. For example, when scattering from both the background and secondary aerosol (i.e., $\sigma_{sca}^{B} + \sigma_{sca}^{S}$) are large, ω_{obs} responds weakly to source inputs of absorbing aerosol. This is because σ_{sca}^{P} and σ_{abs}^{P} are comparably small and thus have a small influence on the overall single scatter albedo. In contrast, when $\sigma_{sca}^{B} + \sigma_{sca}^{S}$ is small, ω_{obs} responds strongly to the same source inputs, especially for strongly absorbing inputs. The dependence of ω_{obs} on ω_P is also an important consideration; we find that ω_P determines the limit of ω_{obs} at high σ_{abs}^{obs} (see Figure S1).

3. Results and Discussion

[8] Considering now the NEAQS 2004 observations within the above framework, quantitative information on the nature of both the regional background aerosol and the primary aerosol source can be extracted by fitting the

observations to equation (2). Not surprisingly, the extensive properties σ^B_{sca} and σ^S_{sca} vary strongly from event to event. There is comparably less variability in the intensive properties ω_B and ω_P, with campaign averages derived from the 50+ events of $\omega_{B,ave} = 0.94 \pm 0.05$ and $\omega_{P,ave} = 0.24 \pm 0.27$ (see Figure S2). We also find that the primary emissions are highly absorbing while the regional background aerosol is mostly scattering, with $\omega_{B,ave}$ equal to the NEAQS campaign average for the sub-micron aerosol [*Sierau et al.*, 2006]. The distribution of ω_p's may be bimodal; however, most event periods (85%) have $\omega_P < 0.4$, and if only these events are considered $\omega_{P,Ave}$ decreases to 0.15 ± 0.16 (Figure S2).

[9] The low average value for ω_P provides strong evidence that the predominant source of sub-micron primary aerosol was combustion. The albedo of primary aerosol produced from diesel engines is similar to $\omega_{P,ave}$ ($\omega_{diesel} \sim 0.2$) [*Ban-Weiss et al.*, 2008]. Significantly larger ω have been observed for primary aerosol from various biomass burning sources [*Lewis et al.*, 2008]. Thus, our results indicate the major inputs of primary aerosol to the marine boundary layer during NEAQS 2004 are from combustion of fossil fuels, consistent with the study area being off the East Coast of the U.S. during the summer and with other estimates from airborne measurements [e.g., *Novakov et al.*, 1997; *Thornhill et al.*, 2008].

[10] The comparably higher ω of the regional background aerosol results from long-time processing of earlier primary aerosol inputs. For older air masses, the variability in source inputs, which gives rise to the range of observed absorption, will be smoothed from diffusion, further entrainment of background air, mixing with other air masses and secondary formation, eventually becoming part of the regional background [e.g., *Abel et al.*, 2003]. As such, observation of a relationship between ω_{obs} and σ^{obs}_{abs} provides a good indication of periods where source information is retained.

[11] Clarke et al. suggested that particle size has an important influence on the observed relationship between ω and σ_{abs}, with larger ω values corresponding to larger particles for a given σ_{abs} [*Clarke et al.*, 2007]. Similarly, we find some correspondence between the particle size (as indicated through the Angstrom exponent for scattering) and ω_{obs} for a given σ_{abs} (see auxiliary material). However, our results indicate that the relative amounts of (weakly absorbing) regional background and secondary aerosol compared to new inputs of (strongly absorbing) primary aerosol from combustion sources is also an important factor in determining the observed ω for a given σ_{abs}.

[12] One event of interest occurred on August 9 when *RHB* was located in Boston Harbor and ω_{obs} ranged from >0.9 to as low as 0.5 (Figure 1c, blue trace). There was a strong correlation between σ^{obs}_{abs} and $[SO_2]_{(g)}$ ($R^2 = 0.84$), implicating ship emissions in the Harbor as an important contributing source. Additionally, the gas-phase [Toluene]/[Benzene] was among the highest of the campaign, indicating that the air mass had undergone little photochemical ageing. A fit to equation (2) yields $\omega_P = 0.19$, $\omega_B = 0.94$ and $\sigma^B_{sca} = \sigma^S_{sca} = 5.7\ Mm^{-1}$ (see below).

[13] One of the few high ω_P events, from the morning of July 14, exhibited very different behavior with respect to the typical ω_{obs} and σ^{obs}_{abs} event relationship (Figure 1c, red trace). During this event the winds were from nearly due east, and the FLEXPART footprint PES indicates that there was no recent contact with local sources. However, the air sampled at this particular time was impacted by forest fires in Alaska and Canada approximately 10 days prior [*Quinn et al.*, 2006; *Warneke et al.*, 2006]. *Warneke et al.* [2006] suggest that the source contributions to the CO burden during this period are split approximately 50:50 between biomass burning and anthropogenic emissions. Consistent with this, the observed increase in ω_{obs} with increasing σ^{obs}_{abs} suggests that the air during this period can be described as the mixing between two distinct aged air masses with similar ω's but with somewhat different absorbing aerosol amounts. The best fit to the observations yields $\omega_P = 0.96$ and $\omega_B = 0.92$.

[14] The Yukon Territory, where much of the biomass burning aerosol likely originated [*Quinn et al.*, 2006], is boreal forest dominated by pine trees. Wood smoke aerosol from various pines has an ω that is large compared to fossil fuel combustion ($\sim$0.9 vs. $\sim$0.2), although we note that ω for wood smoke aerosol depends importantly on the particular fuel type [*Lewis et al.*, 2008]. Thus, the high ω_P for this period may be representative of the primary biomass emissions despite the ca. 10 days transit time. Regardless, these results indicate that optical properties of biomass burning primary emissions can be directly determined by sampling downwind of a burn area and interpreting the observations through equation (2). Other event periods which had notable contributions from biomass burning had recently passed directly over the Boston area and were dominated by interaction with this local source of primary aerosol, thereby precluding determination of the albedo of the biomass burning aerosol (Figures 1c and S4).

[15] Our results can also be used to estimate the fraction of the total observed extinction due to primary emissions during an event as:

$$f^P_{ext} = \frac{\langle \sigma^{obs}_{abs} \rangle + \langle \sigma^{obs}_{abs} \rangle \omega_P/(1-\omega_P)}{\langle \sigma^{obs}_{abs} \rangle + \langle \sigma^{obs}_{abs} \rangle \omega_P/(1-\omega_P) + \sigma^S_{sca} + \sigma^B_{sca} + \sigma^B_{sca}(1-\omega_B)/\omega_B}, \quad (3)$$

where $\langle \sigma^{obs}_{abs} \rangle$ is the mean value of the observed absorption during a given event (see auxiliary material). Because the background contributes some amount to σ^{obs}_{abs}, f^P_{ext} is an upper limit. On average, only a small fraction of the total extinction was due to primary emissions, with $f^P_{ext} = 0.11 \pm 0.16$. The fraction of the sub-micron particle mass from primary emissions can be estimated from f^P_{ext}. Assuming the extinction cross section for the primary emissions is twice that of the background and secondary aerosol (reasonable given the large contribution of black carbon to the primary aerosol), then $f^P_{mass} \sim 0.06$ (this depends explicitly on the assumed ω_p and ω_B). The events on 8/9 (fresh urban/ship emissions) and 7/14 (biomass influenced) discussed above stand out as having particularly high f^P_{ext} of 0.40 and 0.69, respectively. This optical estimate of f^P_{mass} is quantitatively consistent with an estimate derived from chemical composition measurements made during NEAQS (see auxiliary material) and with measurements made along the East Coast during previous campaigns [*Novakov et al.*, 1997; *Magi et al.*, 2005].

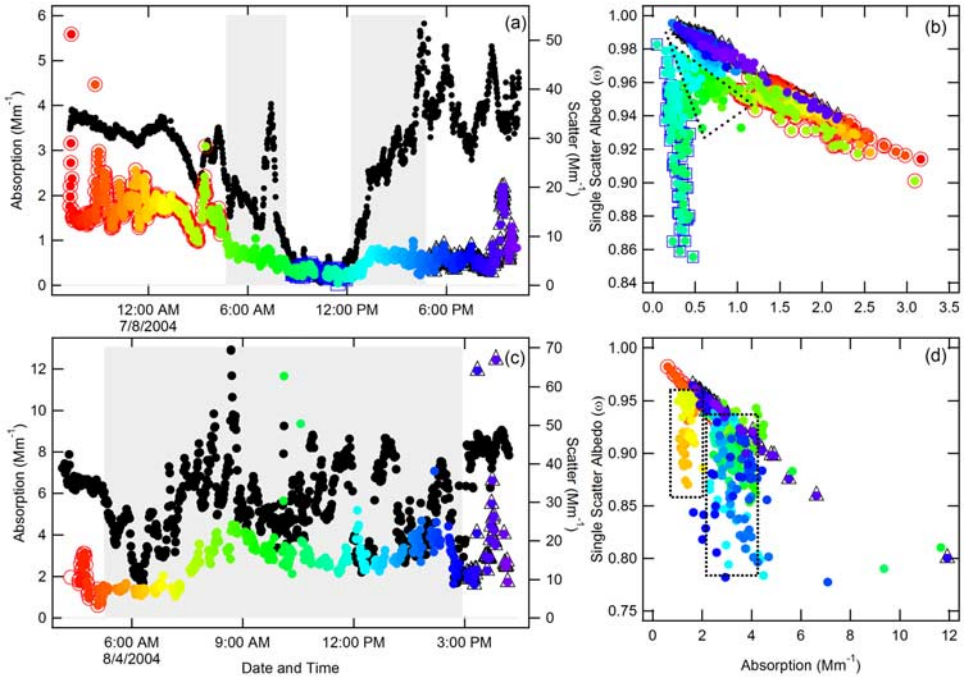

Figure 2. Examples of non-event or between-event behavior. (a and c) show the time series of measured light absorption and scattering (black). Absorption is color coded by time. Periods which were identified as events are also shown as open symbols. Non-event periods are indicated by the gray background. (b and d) show ω_{obs} vs. σ_{abs}^{obs} for the time periods in Figures 2a and 2c, respectively. Figure 2b is representative of a short between-event period where the strong relationship between ω_{obs} and σ_{abs}^{obs} observed during events is temporarily lost. Figure 2d is representative of a longer non-event period. The dotted boxes highlight the non-event behavior.

[16] Although we suggest that the observed scattering can be partitioned into regional background, primary source and secondary aerosol contributions, we find that the fits to equation (2) are not robust with respect to either σ_{sca}^{B} or σ_{sca}^{S} individually, but only to the sum of the two. For example, if we initialize the fit assuming $\sigma_{sca}^{B} = \sigma_{sca}^{S}$, the fit usually returns $\sigma_{sca}^{B} = \sigma_{sca}^{S}$. This result arises from the form of equation (2), which, in the limit of $\omega_{\text{B}} \rightarrow 1$, depends on $\sigma_{sca}^{B} + \sigma_{sca}^{S}$ and not the individual values. Thus, it is not possible to distinguish between the absolute contributions from the regional background and secondary formation to the observed scattering.

[17] Given this sensitivity to initial conditions for the scattering, it is also important to consider how initial conditions affect ω_{P}. Unlike with scattering, the initial choice of ω_{P} had no significant influence on the final best-fit ω_{P} (determined by comparing initial ω_{P} guesses of 0.2 and 0.9). The exception to this was the aged biomass burning event on 7/14, although a good fit was still obtained when the initial fit parameters were judiciously selected (Figure 1c).

[18] Another limitation to the method developed here is that we have assumed both σ_{sca}^{B} and σ_{sca}^{S} are constants in equation (2). While this seems reasonable for the regional background, the amount of secondary aerosol is likely to vary with photochemical age. If the photochemical age varies significantly during event periods then equation (2) may not adequately describe the observed behavior. Visual inspection of the [Toluene]/[Benzene] ratio indicates that the photochemical age during individual events did not tend to vary greatly, thus providing added confidence in our interpretation. (Quantitative comparison is not possible since [Toluene]/[Benzene] is derived from measurements made only every 30 minutes). This complication should be kept in mind if airborne measurements are considered within this framework, as a plane can rapidly sample air masses influenced by a distinct primary aerosol source at very different downwind distances (and therefore lifetimes).

[19] One final consideration is the behavior of ω_{obs} and σ_{abs}^{obs} during "non-event" periods. First, we note that the identification of events is qualitative and therefore biased somewhat towards periods which exhibit a relatively strong variation between ω_{obs} and σ_{abs}^{obs}. Thus, it is likely that the number of events is underestimated. Nonetheless, there were certainly numerous non-event periods observed. In general, these non-event periods were of two types. The first type is generally short in duration and acts to connect two events which occur close in time (Figure 2a). The second type is those which were sustained over relatively long time periods, i.e., having ca. the same duration as an average event (Figure 2b). These non-event periods are likely indicative of locally complex meteorology or larger-scale shifts in the predominant wind direction. Additionally, non-event periods may arise when the ship travels from one location to another, effectively moving in and out of different air masses. During such periods the relationship between ω_{obs} and σ_{abs}^{obs} breaks down because there is no longer a clear delineation between primary source and background. The ship tracks and FLEXPART footprint PES images together suggest that the non-events from

Figure 2a result in large part from movement of *RHB* while the non-event in Figure 2b is from a large-scale shift in the primary source region.

4. Conclusions

[20] We have developed a tool in which the relationship between an intensive (ω_{obs}) and extensive (σ_{abs}^{obs}) aerosol optical property can be used to identify unique air mass "events". These events have been interpreted as having distinct inputs of absorbing primary aerosol to a regional background air mass, and provide a definition of an air mass based on optical boundaries. We have tested this idea using measurements of aerosol optical properties made onboard a ship during NEAQS 2004, where such events were found to occur for at least 1/3 of the total measurement period. The duration of these events was only a few hours on average likely owing to the proximity to local sources coupled with shifts in wind direction and movement of the ship.

[21] Our results indicate that the observed relationship between ω_{obs} and σ_{abs}^{obs} can be generally used to characterize the single scatter albedo of the primary source and regional background aerosol. For NEAQS 2004, the campaign average ω values were 0.23 ± 0.27 and 0.95 ± 0.05 for the primary source and background aerosol, respectively. The low albedo of the primary aerosol and the proximity of the study area to the urban Boston area suggest that emissions from fossil fuel burning were the dominant source of primary aerosol for the majority of the campaign, consistent with previous estimations [e.g., *Novakov et al.*, 1997; *Magi et al.*, 2005]. In addition, the measurements provide an estimate of the fraction of extinction (or particle mass) due to primary emissions. Primary emissions during NEAQS appear to account for only a small fraction of the sub-micron aerosol extinction and mass.

[22] The results presented here indicate another way in which optical property measurements can be used to provide new understanding of primary source inputs to the atmosphere. The large frequency of time periods which correspond to "events" suggests that this is a phenomenon which will be observable in many other environments. Of particular interest for future studies will be a focus on regions which are further from strong anthropogenic sources, regions rich in biomass burning aerosol or dust aerosol and regions with higher emissions of non-combustion derived primary aerosol emissions. The ability to estimate the fractional contribution of primary emissions to the sub-micron extinction provides a variable against which models can be tested. In addition, we suspect that the observed relationship between ω_{obs} and b_{abs}^{obs} will provide a useful new metric against which to test global and regional models and their representations of the spatial and temporal variation in aerosol distributions.

[23] **Acknowledgments.** We thank Carsten Warneke and Joost de Gouw for the VOC data and Andreas Stohl for the FLEXPART maps.

References

Abel, S. J., J. M. Haywood, E. J. Highwood, J. Li, and P. R. Buseck (2003), Evolution of biomass burning aerosol properties from an agricultural fire in southern Africa, *Geophys. Res. Lett.*, *30*(15), 1783, doi:10.1029/2003GL017342.

Ban-Weiss, G. A., et al. (2008), Long-term changes in emissions of nitrogen oxides and particulate matter from on-road gasoline and diesel vehicles, *Atmos. Environ.*, *42*(2), 220–232, doi:10.1016/j.atmosenv.2007.09.049.

Clarke, A., et al. (2007), Biomass burning and pollution aerosol over North America: Organic components and their influence on spectral optical properties and humidification response, *J. Geophys. Res.*, *112*, D12S18, doi:10.1029/2006JD007777.

Draxler, R. R., and G. D. Rolph (2003), HYSPLIT (HYbrid Single-Particle Lagrangian Integrated Trajectory) model, http://www.arl.noaa.gov/HYSPLIT_info.php, Air Resour. Lab., NOAA, Silver Spring, Md.

Ghan, S. J., and S. E. Schwartz (2007), Aerosol properties and processes: A path from field and laboratory measurements to global climate models, *Bull. Am. Meteorol. Soc.*, *88*(7), 1059–1083, doi:10.1175/BAMS-88-7-1059.

Hansen, J., M. Sato, and R. Ruedy (1997), Radiative forcing and climate response, *J. Geophys. Res.*, *102*(D6), 6831–6864, doi:10.1029/96JD03436.

Intergovernmental Panel on Climate Change (2007), *Climate Change: The Physical Science Basis. Contribution of Working Group I to the Fourth Assessment Report of the Intergovernmental Panel on Climate Change*, edited by S. Solomon et al., 996 pp., Cambridge Univ. Press, Cambridge, U. K.

Lewis, K., W. P. Arnott, H. Moosmüller, and C. E. Wold (2008), Strong spectral variation of biomass smoke light absorption and single scattering albedo observed with a novel dual-wavelength photoacoustic instrument, *J. Geophys. Res.*, *113*, D16203, doi:10.1029/2007JD009699.

Magi, B. I., et al. (2005), Aerosol properties and chemical apportionment of aerosol optical depth at locations off the U. S. east coast in July and August 2001, *J. Atmos. Sci.*, *62*(4), 919–933, doi:10.1175/JAS3263.1.

Novakov, T., D. A. Hegg, and P. V. Hobbs (1997), Airborne measurements of carbonaceous aerosols on the east coast of the United States, *J. Geophys. Res.*, *102*(D25), 30,023–30,030, doi:10.1029/97JD02793.

Quinn, P. K., et al. (2006), Impacts of sources and aging on submicrometer aerosol properties in the marine boundary layer across the Gulf of Maine, *J. Geophys. Res.*, *111*, D23S36, doi:10.1029/2006JD007582.

Sierau, B., D. S. Covert, D. J. Coffman, P. K. Quinn, and T. S. Bates (2006), Aerosol optical properties during the 2004 New England Air Quality Study–Intercontinental Transport and Chemical Transformation: Gulf of Maine surface measurements—Regional and case studies, *J. Geophys. Res.*, *111*, D23S37, doi:10.1029/2006JD007568.

Stohl, A., et al. (2005), Technical note: The Lagrangian particle dispersion model FLEXPART version 6.2, *Atmos. Chem. Phys.*, *5*, 2461–2474.

Thornhill, K. L., et al. (2008), The impact of local sources and long-range transport on aerosol properties over the northeast US region during INTEX-NA, *J. Geophys. Res.*, *113*, D08201, doi:10.1029/2007JD008666.

Warneke, C., et al. (2006), Biomass burning and anthropogenic sources of CO over New England in the summer 2004, *J. Geophys. Res.*, *111*, D23S15, doi:10.1029/2005JD006878.

T. S. Bates and P. K. Quinn, Pacific Marine Environmental Laboratory, NOAA, 7600 Sand Point Way NE, Building 3, Seattle, WA 98115, USA. (cdcappa@ucdavis.edu)

C. D. Cappa, Department of Civil and Environmental Engineering, University of California, 1 Shields Avenue, Davis, CA 95616, USA.

D. A. Lack, Chemical Sciences Division, Earth Systems Research Laboratory, NOAA, 325 Broadway, Boulder, CO 80304, USA.